THE JOURNAL OF BIOLOGICAL CHEMISTRY VOL. 281, NO. 10, pp. 6227–6235, March 10, 2006

Blockade of NFAT Activation by the Second Calcineurin Binding Site*

Received for publication, December 29, 2005 Published, JBC Papers in Press, January 6, 2006, DOI 10.1074/jbc.M513885200

Sara Martínez-Martínez[‡1], Antonio Rodríguez[§1], Maria Dolores López-Maderuelo[‡§], Inmaculada Ortega-Pérez[‡2], Jesús Vázquez[§], and Juan Miguel Redondo[‡§3]

From the [‡]Centro Nacional de Investigaciones Cardiovasculares (CNIC) , Melchor Fernández Almagro 3, 28029 Madrid, Spain and the [§]Centro de Biología Molecular Severo Ochoa, Consejo Superior de Investigaciones Científicas (CBM-CSIC), Universidad Autónoma de Madrid (UAM) , Facultad de Ciencias, 28049 Madrid, Spain

Activation of NFAT transcription factors requires their dephosphorylation by the phosphatase calcineurin (CN). NFATs contain two CN binding motifs: PxIxIT and CnBP-B/CNBR2 (which we call LxVP). Here we carry out a detailed comparative analysis of the CN binding activity displayed by the PxIxIT and LxVP sites from different NFATs. Dose-response CN binding experiments with GST fusion proteins of NFATc1 and NFATc2 showed that NFATc1 binds CN *in vitro* more efficiently than does NFATc2. This difference in binding appears to be caused by the different CN binding potencies of the corresponding LxVP sites; thus while the LxVPc2 peptide fused to GST did not bind CN, GST-LxVPc1 bound it more efficiently than did GST-PxIxITc1 or GST-PxIxITc2. Furthermore, an NFATc2 chimera protein containing the LxVP motif from NFATc1 interacted with CN much more potently than did wild-type NFATc2. Free peptides spanning the LxVP motifs from NFATc1, c3 or c4 displaced CN from GST-NFATc1 and GST-NFATc2 more efficiently than any PxIxIT peptide. PxIxITc2 and LxVPc1 peptides were each able to cross-compete GST-LxVPc1-CN and GST-PxIxITc2-CN binding. In contrast with PxIxITc2, the LxVP peptide not only blocked CN-NFAT binding but also inhibited CN phosphatase activity *in vitro*. Furthermore, exogenous LxVPc1 blocked NFATc2 phosphorylation and nuclear translocation *in vivo*. These results suggest a model in which the different CN binding characteristics of the PxIxIT and LxVP sites enable different NFAT members to influence each others activities in cells where they are co-expressed.

The calcium/calcineurin/NFAT pathway plays a pivotal role in many important biological processes, including the development and function of the immune and nervous systems, patterning of the vasculature, heart valve morphogenesis, and muscle growth and development (1–5). Calcium signals activate the phosphatase calcineurin (CN),[4] which dephosphorylates the transcription factors NFATc1, NFATc2, NFATc3, and NFATc4 (HUGO nomenclature). This induces their translocation from the cytosol to the nucleus and DNA binding activity, and thus promotes NFAT-dependent gene expression (6). Binding of NFATs by CN is thus a key step in the activation of this transcription factor family.

Calcineurin, also known as protein phosphatase 2B, is a heterodimer consisting of a catalytic subunit (CnA) tightly bound to a regulatory subunit (CnB). CnA is composed of a catalytic domain and a regulatory domain that contains a CnB binding sequence, a calmodulin (CaM) binding domain and an autoinhibitory segment (7). The phosphatase activity of CnA is regulated by a complex formed by Ca^{2+} and CnB and CaM; and both regulatory proteins are essential for activity (7, 8). CN can bind both to phosphorylated and to dephosphorylated NFATs (9, 10), and although non-activated CN can bind NFATs, the binding interaction is stronger with activated CN (11). In NFATs, this interaction has been mapped within the N-terminal regulatory domain, which is conserved in all four members (12–14). A mutational analysis of the conserved motifs within the regulatory domain of NFATc2 defined the sequence SPRIEIT as a calcineurin docking site (15). Subsequent studies identified the residues conserved in corresponding sequences from other NFAT proteins, and defined the PxIxIT motif (see Fig. 1*A*), which appears to be functional in all the CN-regulated NFAT members (11, 16–18).

NFAT was originally identified in T lymphocytes as a factor essential for *IL-2* gene expression (19), and was subsequently implicated in the regulation of many other genes necessary for an effective immune response (20–23). The finding that CN is the intracellular target of clinically important immunosuppressive drugs such as cyclosporin A (CsA) and FK506 (24) further highlighted the importance of the calcium/CN/NFAT pathway and the particular importance of NFATs in the immune system (25–27). Given the side effects associated with CsA and FK506, the use of these drugs is limited to severe clinical situations such as organ transplantation. The inhibition of CN activity against substrates other than NFAT has been proposed as a cause of the deleterious effects of these drugs. For this reason, specific disruption of the CN-NFAT interaction has attracted interest as a potentially novel way to inactivate NFATs more selectively (28). Such a profile has been reported for VIVIT, a high affinity CN-binding peptide based on the PxIxIT consensus sequence (29), and for INCA small organic molecules (30). Both types of molecule were described as specific NFAT inhibitors on the basis of their ability to disrupt the CN-NFAT interaction whereas having no effect on CN-mediated activation of other substrates.

More recently, independent studies on NFATc3 and NFATc1 identified a second CN recognition site close to the C-terminal region of the regulatory region, named CNBR2 and CnBP-B, respectively (17, 31). Analysis of the primary sequence of this motif in CN-regulated NFAT proteins identified a conserved LxVP sequence present in all members. To be consistent with the nomenclature used for the PxIxIT CN dock-

* This work was supported by Grants SAF2003-02920 from MCYT, Grants LSHM-CT-2004-005033 (EICOSANOX) from the European Union, Centro Nacional de Investigaciones Cardiovasculares, Fundació La Marató from TV3, and RECAVA from Ministerio de Sanidad y Consumo from Spain (to J. M. R.), and by Grants CICYT BIO2003-01805 and CAM GR/SAL/0141/2004 (to J. V.). The costs of publication of this article were defrayed in part by the payment of page charges. This article must therefore be hereby marked "*advertisement*" in accordance with 18 U.S.C. Section 1734 solely to indicate this fact.

[1] Both authors contributed equally to this work, and the order of authorship should be considered arbitrary.

[2] Recipient of a Centro Nacional de Investigaciones Cardiovasculares fellowship.

[3] To whom correspondence should be addressed: Centro Nacional de Investigaciones Cardiovasculares (CNIC), Melchor Fernández Almagro 3, Madrid 28029, Spain. Tel.: 34-91-497-8270; Fax: 34-91-497-4799; E-mail: jmredondo@cbm.uam.es.

[4] The abbreviations used are: CN, calcineurin; GST, glutathione *S*-transferase; PBS, phosphate-buffered saline; GFP, green fluorescent protein; HA, hemagglutinin; CaM, calmodulin; CsA, cyclosporin A.

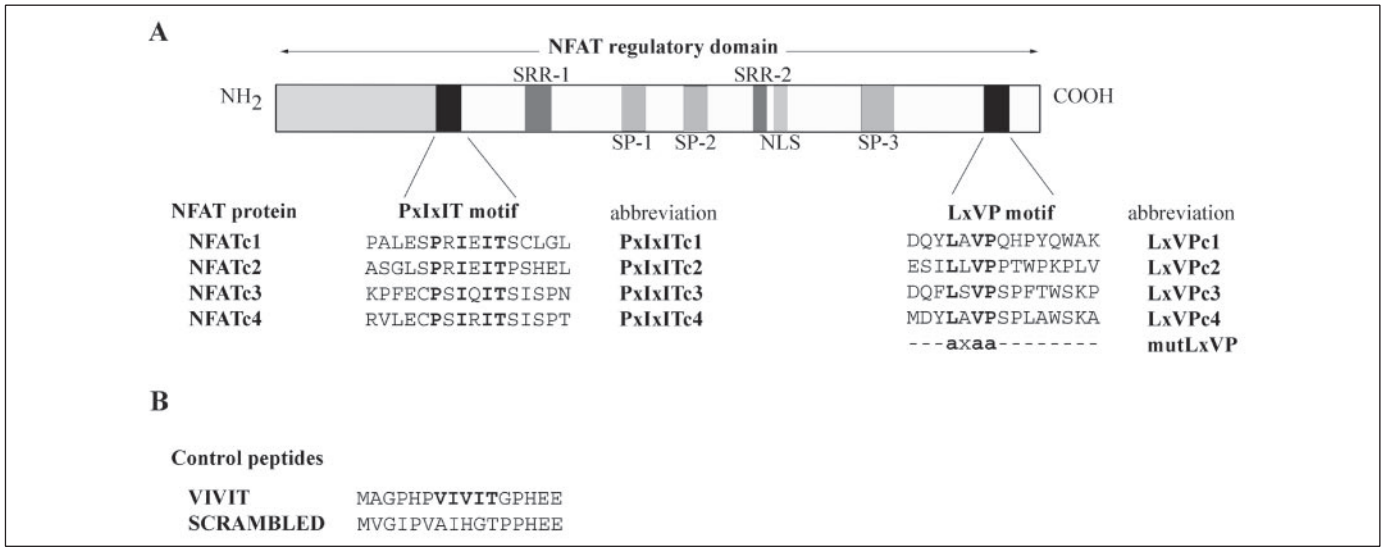

FIGURE 1. *A*, schematic representation of the N-terminal regulatory domain and the CN-interacting sequences of the NFAT proteins. The conserved regions among the different NFAT members are detailed as follows: *SP-1*, *SP-2*, and *SP-3* are serine-proline repeat motifs susceptible to phosphorylation; *SRR-1* and *SRR-2* are serine-rich regions; and *NLS* is a nuclear localization signal. The two regions involved in binding CN, labeled as PxIxIT and LxVP motifs, are shown in *black*, and the sequences underneath show the regions corresponding to these motifs from the four human NFAT members; amino acids conserved among all members are shown in *bold*. The indicated residues were replaced by alanines to generate the corresponding mutant LxVPc1 peptide. The abbreviations used for the different PxIxIT and LxVP motifs are shown on the *right*. *B*, amino acid sequences corresponding to the control peptides used as positive (VIVIT) or negative (SCRAMBLED) competitors for *in vitro* binding experiments.

ing site, we therefore refer to this second site as the LxVP motif (see Fig. 1*A*). Deletional analysis of NFATc3 followed by binding competition assays delimited the minimal LxVP motif required for direct CN binding to a 16-amino acid region: DSSGDQFLSVPSPFTW (31, 32). Similar deletional analysis mapped the minimal LxVP CN binding site of the NFATc1 regulatory domain to the homologous sequence DQYLAVPQHPYQWAK (17).

Although these previous studies shed some light on the importance of these CN binding sites in different NFAT members, their binding characteristics have not been fully characterized. The experiments we present in this report constitute the first detailed evaluation of the relative CN binding activity of the different PxIxIT and LxVP motifs to CN-NFAT binding. Given that NFATc1 and NFATc2 are co-expressed in several cell types (33–38), we have investigated whether the LxVP region of each was relevant to their respective binding to CN. Our experiments show that NFATc1 interacts with CN more strongly than NFATc2, and that the NFATc1 LxVP motif (LxVPc1) binds CN more efficiently than do any of the PxIxIT motifs. We further found that a chimeric NFATc2 protein containing the LxVPc1 motif binds to CN more strongly than does wild-type NFATc2. Moreover, even though the NFATc2 LxVP motif makes little contribution to NFATc2 binding to CN, the peptide corresponding to the NFATc1 LxVP motif is able specifically to prevent NFATc2 activation by blocking its binding to CN and inhibiting its phosphatase activity. These results provide new insights into the CN-NFAT interaction.

EXPERIMENTAL PROCEDURES

Plasmids—The GST-NFATc1 construct expressing the regulatory region of NFATc1 (1–418 amino acids) fused to glutathione *S*-transferase (GST) was generously provided by Dr. A. Rao (12). GST-NFATc2 was generated by in-frame subcloning of the cDNA sequence encoding amino acids 4–385 of NFATc2 into the BamHI-SmaI-digested pGEX4T3 vector (Amersham Biosciences). The GST-NFATc2ΔLxVP construct was generated by fill-in of the EcoRI unique site located upstream the LxVPc2 motif, adding an in-frame stop codon. To generate GST-NFATc1ΔLxVP we first carried out site-directed mutagenesis to generate a second EcoRI site located upstream the LxVPc1 motif (hNFATc1 G381E mutant). This new construct, which contains two EcoRI sites flanking the LxVP sequence, was EcoRI-digested to excise the LxVP motif, and the remaining plasmid was re-ligated. The GST-NFATc2-LxVPc1 swap mutant was generated by in-frame cloning of an annealed double-stranded oligonucleotide encoding the LxVPc1 motif into the EcoRI/SalI-digested pGEX-NFATc2 construct.

The GST-peptide constructs and GFP-peptide expression vectors were generated by in-frame cloning of the annealed double-stranded overhang oligonucleotides encoding the different peptide sequences into restriction enzyme-digested pGEX (Amersham Biosciences) or pEGFP-C plasmids (Clontech). The sequences of the oligonucleotides used were: VIVIT forward, 5′-tcgagcatggcaggtccacatccagtcatcgttatcaccggtccacatgaggaaggcggacc-3′; VIVIT reverse, 5′-catgggtccgccttcctcatggtggaccggtgataacgatgactggatgtggacctgccatgc-3′; PxIxITc1 forward, 5′-agcttggccaccatgccggcgttggaaagcccacggatagagattacgagttgcttgggattg-3′; PxIxITc1 reverse, 5′-gatccaatcccaagcaactcgtaatctctatccgtgggctttccaacgccggcatggtggcca-3′ LxVPc1 forward, 5′-tcgagcgatcagtacttggccgtaccacagcatccgtatcaatgggctaaggg-3′; LxVPc1 reverse 5′-aattcccttagcccattgatacggatgctgtggtacggccaagtactgatcgc-3′; mutLxVPc1 forward, 5′-agcttggccaccatggatcagtatgcggcagctgcccagcatccgtatcaatgggcgaag-3′; mutLxVPc1 reverse, 5′-gatccttcgcccattgatacggatgctgggcagctgccgcatactgatccatggtggcca-3′; PxIxITc2 forward, 5′-gatctgccaccatggcgagtgggttgagcccgaggatagagataacgccgagtcatgagttag-3′; PxIxITc2 reverse, 5′-gatcctaactcatgactcggcgttatctctatcctcgggctcaacccactcgccatggtggca-3′; LxVPc2 forward, 5′-agcttggccaccatggagagcatcctgctagtacctccgacctggcctaagccgttggtg-3′; LxVPc2 reverse, 5′-gatccaccaacggcttaggccaggtcggaggtactagcaggatgctctccatggtggcca-3′.

The expression plasmid pEF-BOS HA-NFATc2 has been described previously (39), and encodes the full-length NFATc2 with the influenza virus hemagglutinin (HA) epitope at its N-terminal region.

Cell Transfections and Western Blotting of Cell Extracts—HeLa cells were cultured in Dulbecco's modified Eagle's medium (Invitrogen) supplemented with 10% fetal bovine serum (Sigma). Cells were plated on 6-well plates the day before transfection so that they reached 80% confluence on the day of transfection. Cells were transfected with 18 ng of

pEF-BOS HA-NFATc2 plus 1.1 μg of GFP-based expression plasmids with 4 μl of Plus reagent plus 6 μl of Lipofectamine reagent (Invitrogen) for 3 h in 1 ml of OPTIMEM medium (Invitrogen). Flow cytometry was used to monitor the transfection efficiencies as the percentage of GFP-expressing cells. Similar transfection efficiencies of the different constructs were found in independent experiments.

Twenty-four hours after transfection, the culture medium from HeLa-transfected cells was replaced by Dulbecco's modified Eagle's medium supplemented with 1% fetal bovine serum. Two hours later, cells were stimulated with 20 ng/ml phorbol 12-myristate 13-acetate (PMA) (Sigma) plus 1 μM calcium ionophore A23187 (Sigma) and 3 mM $CaCl_2$ for 1 h. Cells were then washed with ice-cold phosphate-buffered saline (PBS), and lysed with lysis buffer (20 mM Hepes pH 7.6, containing 0.4 M NaCl, 1 mM EDTA, 3 mM EGTA, 1 μM dithiothreitol, 1 mM phenylmethylsulfonyl fluoride, 100 μM benzamidine, 1 μg/ml of pepstatin, 1 μg/ml of aprotinin, and 1% Triton X-100). The cellular proteins from suspended cells were extracted during 15 min on a rocking platform, and centrifuged at 14,000 × *g* for 15 min. All steps were performed at 4 °C. After centrifugation, the supernatants were collected, and Laemmli buffer was added. Total cell extracts were boiled for 10 min, loaded onto SDS-polyacrylamide gels (6% for NFAT or 10% for active CN or GFP), and proteins were separated by electrophoresis under reducing conditions. The protein gels were transferred to nitrocellulose membranes and then incubated in blocking solution (10%, w/v skimmed milk in PBS) for 1 h at room temperature. After several washes with PBS-T (0.1% Tween-20 in PBS), the membranes were incubated for 2 h with the corresponding first antibody solution: mouse monoclonal anti-HA antibody 12CA5 (0.05%, v/v) in PBS-T with 1% bovine serum albumin to detect NFATc2; or the rabbit polyclonal anti-GFP serum provided by Dr. I. Crespo (0.1%, v/v) in PBS-T with 5% skimmed milk. Membranes were then washed three times for 5 min each with PBS-T, and incubated with peroxidase-labeled goat anti-mouse IgG (Pierce) or anti-rabbit IgG (Pierce) for 1 h at room temperature. After three washes with PBS-T and one wash with H_2O, membrane-bound antibody was detected with the ECL (enhanced chemiluminescence) detection reagent (Amersham Biosciences).

Immunofluorescence—HeLa cells were transfected as described above with 1.2 μg of GFP-based expression plasmid plus 40 ng of pEF-BOS HA-NFATc2. Two hours before stimulation, the culture medium was replaced by Dulbecco's modified Eagle's medium supplemented with 1% fetal bovine serum. After stimulation for 30 min with calcium ionophore A23187 (1 μM) and $CaCl_2$ (3 mM), cells were fixed for 10 min at room temperature with 10% formaldehyde PBS containing 4% saccharose. They were then washed three times with PBS, and permeabilized with 0.25% Triton X-100 in PBS for 10 min at room temperature. Permeabilized cells were incubated with blocking buffer (10% bovine serum albumin in PBS) for 20 min, followed by 1 h of incubation with a 1:500 dilution of 12CA5 anti-HA. The subcellular localization of NFAT proteins was detected by fluorescence microscopy (Axiovert-200, Zeiss), with goat anti-mouse IgG Alexa 594 (Molecular Probes) as secondary antibody. The percentage of cells with nuclear- or cytosolic-localized NFAT was calculated by scoring at least 130 positive cells per transfection.

In Vitro Calcineurin-NFAT Binding Assays—GST fusion proteins were expressed in the protease-deficient BL21(DE3) *Escherichia coli* strain and were purified with glutathione (GSH)-Sepharose 4B beads (Amersham Biosciences). Calcineurin binding assays, with these GST fusion proteins used to pull-down CN, were carried out as follows. Beads containing GST fusion proteins of NFAT regulatory domains (1–2 μg) or of peptides (10–30 μg) were washed twice with binding buffer (20 mM Tris, pH 8.0, 100 mM NaCl, 1.5 mM $CaCl_2$, 6 mM $MgCl_2$, 1 mM phenylmethylsulfonyl fluoride, 1 μM dithiothreitol, 1 μg/ml of aprotinin, 1 μg/ml of pepstatin, 100 μM benzamidine, and 0.2% Triton X-100) and then incubated with 20 nM calcineurin (Sigma) plus 600 nM calmodulin (Sigma) in binding buffer with or without the corresponding peptide for 30 min on a rocking platform at 4 °C. The experiments shown in Fig. 6*C* were performed using binding buffer without 1.5 mM $CaCl_2$ and in the presence or absence of 600 nM calmodulin. After the incubation, samples were briefly centrifuged at 4 °C. The supernatants were saved, and Laemmli buffer was added to them for later analysis (non-bound fraction). The beads were then washed five times with freshly made ice-cold binding buffer, and the bound proteins were eluted by boiling the samples in Laemmli buffer (bound fraction). Bound and non-bound fractions were loaded onto a 10% SDS-polyacrylamide gel and separated by electrophoresis under reducing conditions. Calcineurin was detected by Western blotting with a mouse monoclonal anti-CnA antibody (clone G182-1847, PharMingen). All of these binding experiments have been repeated, and the results shown are representative of at least three independent experiments. Where indicated, the amount of CN bound to GST fusion protein was quantified densitometrically with Quantity One software (Bio-Rad).

Peptides were synthesized at the Protein Synthesis Facility of the Centro de Biología Molecular Severo Ochoa CSIC-UAM. The amino acid sequences were: VIVIT peptide, MAGPHPVIVITGPHEE; SCRAMBLED peptide, MVGIPVAIHGTPPHEE; PxIxIT from human NFATc1, PALESPRIEITSCLGL; PxIxIT from human NFATc2, ASGLSPRIEITPSHEL; PxIxIT from human NFATc3, KPFECPSIQITSISPN; PxIxIT from human NFATc4, RVLECPSIRITSISPT; LxVP from human NFATc1, DQYLAVPQHPYQWAK; mutated LxVP from human NFATc1, DQYAAAAQHPYQWAK; LxVP from human NFATc2, ESILLVPPTWPKPLV; LxVP from human NFATc3, DQFLSVPSPFTWSKP; LxVP from human NFATc4, MDYLAVPSPLAWSKA.

Calcineurin Phosphatase Activity Assay—The effect of the indicated peptides on CN enzymatic activity was analyzed with the Biomol green calcineurin assay kit (Biomol), in accordance with the manufacturer's instructions. A combination of CsA (Sandoz) plus cyclophilin A (CyP-A) (Sigma) was employed to inhibit the *in vitro* calcineurin activity.

RESULTS

The CN Binding Activity of NFATc1 Is Higher Than That of NFATc2—To analyze the ability of NFATc1 and NFATc2 to interact with CN, we conducted *in vitro* binding experiments. We compared the levels of CN bound to decreasing concentrations of the purified recombinant regulatory domain of NFATc1 or NFATc2 fused to GST protein (GST-NFATc1 and GST-NFATc2, respectively). Densitometric quantification of bound CN in these assays indicated that NFATc1 has a submicromolar binding affinity for CN, and that the affinity of NFATc2 appears to be much lower than that of NFATc1 (Fig. 2*A*).

In complementary experiments the concentration of CN protein was varied. In each case, the amount of CN bound to the GST-NFAT fusion proteins decreased as the concentration of CN was progressively reduced. However, in agreement with the results of varying GST-NFAT concentrations, binding to NFATc1 was stronger than to NFATc2 at each CN concentration used (Fig. 2*B*).

The CN Binding Activity of the LxVPc1 Motif Is Higher Than That of PxIxIT Motifs—This difference in CN binding might arise from the different CN binding potencies of the PxIxIT and LxVP sites from NFATc1 and NFATc2. The second CN-interacting sites show limited

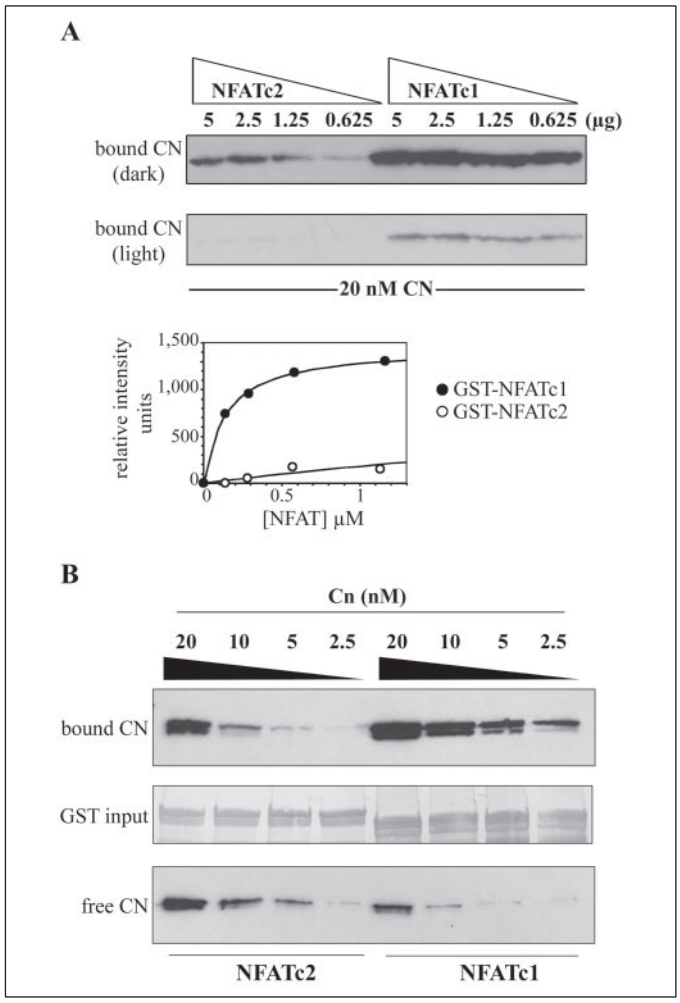

FIGURE 2. **Comparison of CN binding to NFATc1 and NFATc2 *in vitro*.** *A*, dependence of NFATc1 and NFATc2 binding to CN on NFAT concentration. CN (20 nM) was reacted in pull-down assays with decreasing amounts of the regulatory domain of NFATc2 or NFATc1 fused to GST (GST-NFATc2 and GST-NFATc1). Bound CN was visualized by Western blot with a monoclonal anti-CnA antibody. Because of the high amounts of CN bound to NFATc1, two different exposures are shown (*top* and *bottom panels*) to show the NFATc1-CN interaction clearly. Bound CN was quantified densitometrically, and these data, as relative intensity units of CN bound at each NFAT concentration, are presented in the *bottom graphic*. *B*, dependence of CN-NFAT binding on CN concentration. GST-NFATc2 (*left*) or GST-NFATc1 (*right*) was reacted with decreasing concentrations of CN (20, 10, 5, and 2.5 nM CN). CN was detected by immunoblotting with anti-CnA monoclonal antibody: bound CN is shown in the *upper blot*; and the *bottom blot* shows unbound (free) CN in one-third volumes of the postreaction supernatants. Ponceau red staining of the Western blot membranes confirmed equal amounts of GST fusion proteins in reactions (*middle panel*).

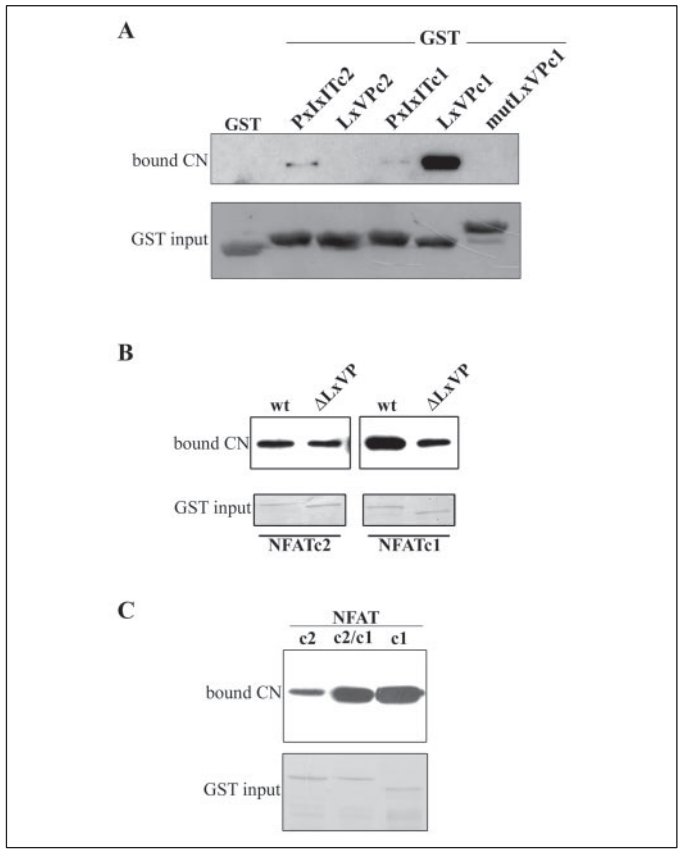

FIGURE 3. **Analysis of the *in vitro* interaction of CN with PxIxIT and LxVP peptides fused to GST and the relevance to CN interaction of the LxVP motif in NFATc1 *versus* NFATc2.** *A*, GST-peptide fusion proteins containing the PxIxIT or LxVP sequences from NFATc1 or NFATc2 were used to pull-down CN. GST protein or GST fused to the mutated LxVPc1 (AxAA) sequence were used as negative controls. Bound CN was detected by Western blot, and even input of GST-peptide fusion proteins was confirmed by staining total protein on SDS-PAGE gels. *B*, comparison between CN binding to wild-type GST-NFAT members (*wt*) and the corresponding LxVP deletion mutant (ΔLxVP) in pull-down assays. The input of GST fusion proteins used in experiments was determined by total protein staining. *C*, GST-NFATc2-LxVPc1 swap mutant (*c2/c1*) was used to pull-down CN, and the amount of CN bound to this mutant protein was compared with that bound to wild-type GST-NFATc2 (*c2*) and GST-NFATc1 (*c1*).

homology among NFAT members, but alignment of the corresponding sequences indicated that three conserved residues (Leu, Val, and Pro) are present in all members (Fig. 1*A*). To test the ability of each PxIxIT or LxVP sequence to interact with CN independently, we generated GST-peptide fusion proteins bearing the PxIxIT and LxVP motifs from NFATc1 and NFATc2 (Fig. 1*A*), and used them in CN binding pull-down experiments (Fig. 3*A*). The amount of CN bound to GST-LxVPc1 was much greater than that bound to GST-PxIxITc1 or GST-PxIxITc2, whereas GST-LxVPc2 was unable to bind CN under the same experimental conditions. The importance of the conserved Leu, Val, and Pro amino acids for the binding activity of LxVPc1 was studied with GST-mutLxVPc1, in which each conserved residue was replaced with alanine (see Fig. 1*A*); GST-mutLxVPc1 was unable to bind CN (Fig. 3*A*). These results suggest that the higher CN binding capacity of the LxVP motif from NFATc1 (relative to the PxIxITc1 and PxIxITc2 motifs) could indeed account for the stronger interaction of CN with NFATc1 *versus* NFATc2. To analyze the contribution of each LxVP motif to the overall binding to CN, we deleted them from GST-NFATc2 and c1 constructs. We found that the CN binding activity of NFATc2 was barely affected by the deletion of its LxVP sequence (Fig. 3*B*). In contrast, removal of the LxVP motif from NFATc1 significantly reduced its binding to CN. To directly demonstrate the participation of the LxVPc1 motif in the binding to CN, we compared the amount of CN bound to an NFATc2-LxVPc1 swap mutant (c2/c1) to that bound to wild-type NFATc2. These experiments clearly showed that the presence of an LxVPc1 motif greatly increased the CN binding activity of NFATc2 (Fig. 3*C*). These results strongly support the idea that the differential CN binding between NFATc1 and NFATc2 is caused by the different CN binding capabilities of their LxVP motifs.

Effects of PxIxIT and LxVP Peptides on the Interaction of NFAT and CN in Vitro—Given the different CN interaction strengths of the PxIxIT and LxVP sites, we tested the ability of the peptides corresponding to these sequences to compete *in vitro* with purified GST-NFATc2 for binding to CN. The synthetic peptides corresponding to the LxVP and PxIxIT CN binding sites from NFATc1 and NFATc2 are shown in Fig. 1*A*. The quantity of CN bound to GST-NFAT was detected by Western blot analysis. In these experiments, the VIVIT peptide (Fig. 1*B*), a

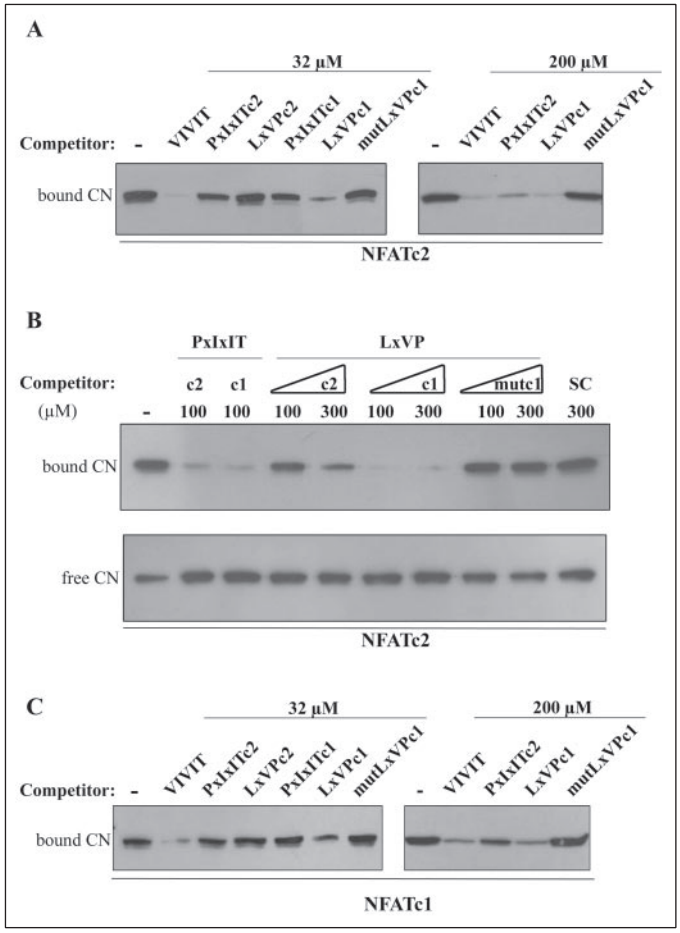

FIGURE 4. **Effects of NFATc2- and NFATc1-derived PxIxIT and LxVP peptides on CN-NFAT interaction *in vitro*.** GST-NFAT-CN binding assays were performed in the presence of the indicated synthetic peptides, and bound CN was detected by Western blot with a monoclonal anti-CnA antibody. *A*, CN bound to GST-NFATc2 in the presence of competitor peptides at 32 μM or 200 μM. The mutLxVPc1 peptide contains the LxVP motif from NFATc1 with the Leu, Val, and Pro residues replaced by alanines. *B*, CN bound to GST-NFATc2 in the presence of high concentrations of competitor peptides. The SCRAMBLED control peptide (*SC*) was used as a negative control. The *lower blot* shows unbound (*free*) CN in one-third volumes of the postreaction supernatants. *C*, CN bound to GST-NFATc1 in the presence of competitor peptides at 32 μM or 200 μM.

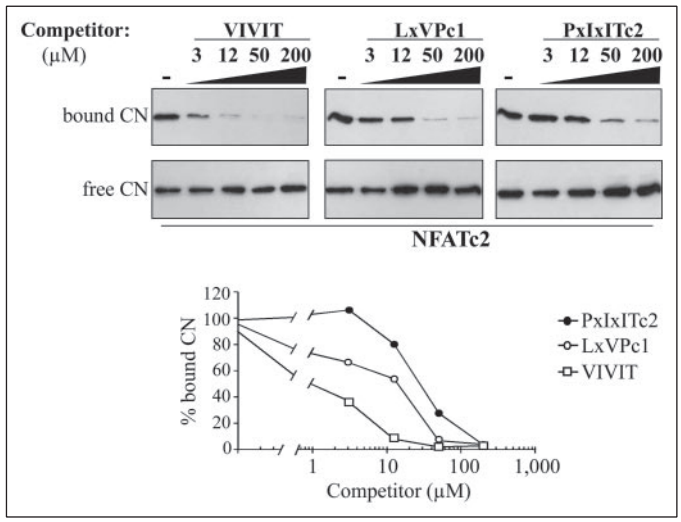

FIGURE 5. **Comparison of the abilities of VIVIT, LxVPc1, and PxIxITc2 peptides to block CN binding to NFATc2.** GST-NFATc2 binding to CN was competed by increasing concentrations of VIVIT, LxVPc1, or PxIxITc2 peptides. The *upper blots* show the amounts of CN bound to GST-NFATc2, and the lower blots show the unbound (*free*) CN in one-third volumes of postreaction supernatants. Bound CN was quantified by densitometric analysis with the Quantity One software, and these data are presented in the graph to show the inhibition curves of each competitor peptide for the binding of CN to GST-NFATc2. 100% bound CN is the amount of CN bound to GST-NFATc2 in the absence of competitor peptide.

sequence highly selected from combinatorial peptide libraries (29), was used as a potent control competitor.

The PxIxIT peptides corresponding to NFATc1 and NFATc2 (PxIxITc1 and PxIxITc2, respectively) were approximately equipotent in displacing NFATc2 from CN (Fig. 4*A*), but there were clear differences between the two corresponding LxVP-based peptides. LxVPc1, the peptide containing the LxVP sequence from NFATc1, disrupted CN binding to NFATc2. This effect was stronger even than that of the PxIxITc2 sequence, which is described as the CN docking site in this NFAT (Fig. 4*A*). In contrast, the same concentration of the NFATc2-specific LxVP peptide (LxVPc2) failed to compete with NFATc2 for binding to CN (Fig. 4*A*, *left panel*). In these experiments mutLxVPc1 peptide did not affect the binding of CN to NFATc2, indicating that these residues are necessary for displacing NFAT from CN *in vitro*.

These results suggested that LxVPc2 does not interact with CN, or more likely that its ability to bind CN is much weaker than that of LxVPc1. To explore this further we increased the concentrations of competitor peptides in the binding reaction. As shown in Fig. 4*B*, whereas 100 μM concentrations of PxIxITc1, PxIxITc2, or LxVPc1 efficiently displaced CN from NFATc2, the LxVPc2 peptide caused only a partial inhibition at high concentrations. The control mutLxVPc1 peptide and a random sequence of the amino acid constituents of the VIVIT peptide (SCRAMBLED) (see Fig. 1*B*) both failed to affect CN binding to NFATc2, even at the highest peptide concentration assayed.

The peptides that disrupted NFATc2-CN binding were also able to inhibit the binding of NFATc1 to CN (Fig. 4*C*). Consistent with the differential CN binding observed for NFATc1 and NFATc2 (Fig. 2), the peptides, even at 200 μM, were less effective at competing for CN binding with NFATc1 than with NFATc2 (Fig. 4*C*). These results further reinforce the hypothesis that the overall affinity of NFATc1 for CN is higher than that of NFATc2.

LxVPc1 Peptide Is a Potent Inhibitor of NFAT Binding to Activated CN—Dose-response competition experiments confirmed that LxVPc1 peptide is more potent than PxIxITc2 at competing the binding of GST-NFATc2 to CN (Fig. 5). In these experiments the amount of bound CN was analyzed by computer-aided quantification of Western blots. The high affinity VIVIT peptide, used as positive control, was the most potent competitor (Fig. 5, *left panel*). LxVPc1 at 50 μM was able to completely block binding, whereas the same concentration of PxIxITc2 exerted only a partial inhibitory effect (Fig. 5, *middle* and *right panels*).

The difference between the inhibitory potencies of the LxVPc1 and LxVPc2 peptides prompted us to extend the study to the LxVP motifs from the other NFAT members. Synthetic peptides corresponding to the LxVP motifs of NFATc1, c3 and c4 inhibited the interaction of CN with GST-NFATc1 or GST-NFATc2 to a similar degree when used at 32 μM (Fig. 6*A*); only LxVPc2 and the mutLxVPc1 negative control failed to disrupt the CN-NFAT interaction at this concentration. In parallel experiments, peptides based on the PxIxIT sequences from all the different NFAT members were used as competitors. As shown in Fig. 6*B*, at 100 μM (three times higher than the concentrations of LxVP peptides used), all the PxIxIT peptides, but not the SCRAMBLED control peptide, blocked the interaction between CN and NFATc1 or NFATc2. Thus of all the peptides corresponding to the two binding sites from the four NFAT family members, only LxVPc2 does not compete efficiently with NFATc1 and NFATc2 for the interaction with CN *in vitro*; and the other LxVP peptides were more effective competitors than the PxIxIT peptides.

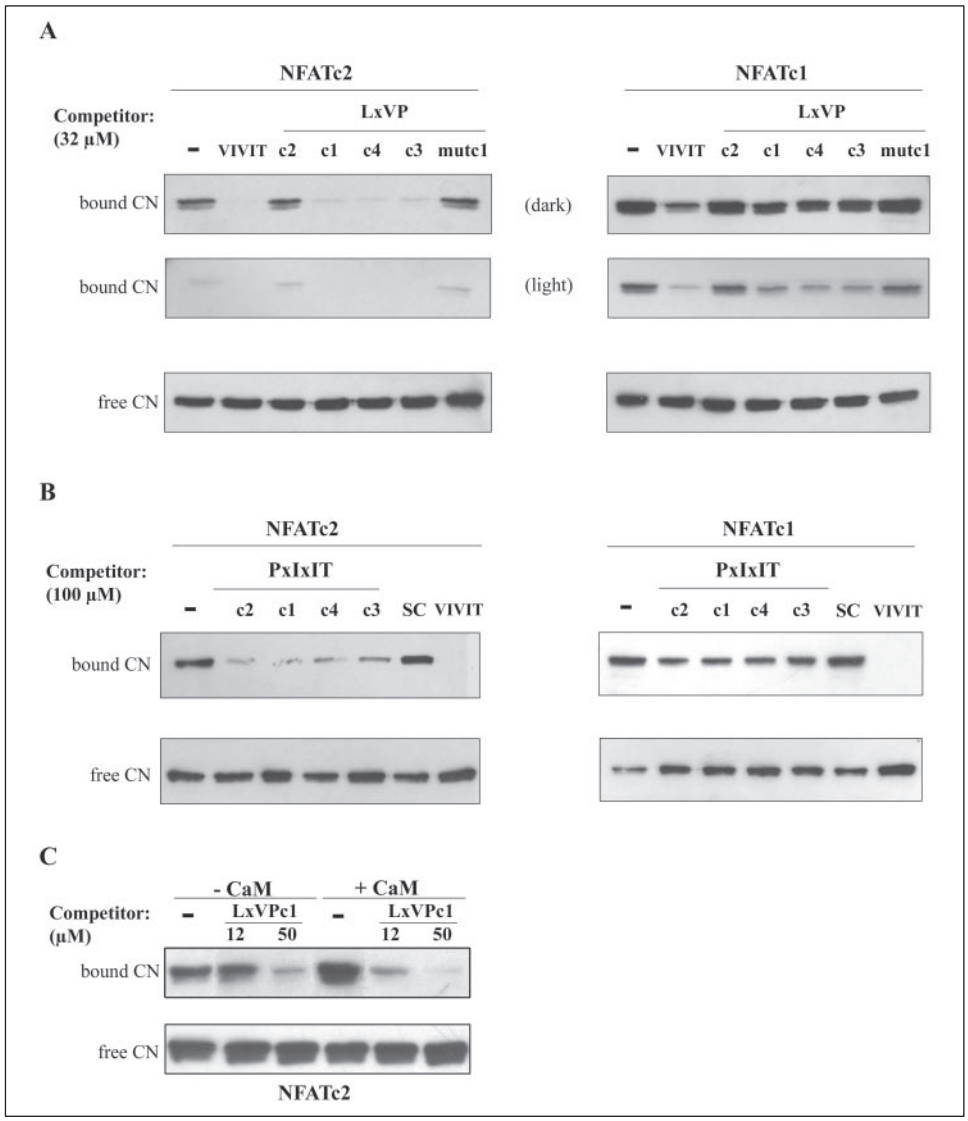

FIGURE 6. **Effective competition of the interaction of NFATc1 and NFATc2 with activated CN with peptides spanning the LxVP motifs of NFATc1, c3, and c4.** *A*, peptides corresponding to the LxVP motifs from NFATc1, c2, c3, or c4 (32 μM) were used to compete *in vitro* for activated CN binding to GST-NFATc2 (*left*) or GST-NFATc1 (*right*). Because of the high amounts of CN bound to NFATc1, two different exposures are shown (*top* and *middle panels*) to show clearly the effect of the peptides on the NFATc1-CN interaction. The *bottom blot* shows the amount of unbound (*free*) CN in one-third volumes of postreaction supernatants. *B*, *in vitro* GST-NFAT-CN binding in the presence of 100 μM of each PxIxIT peptide corresponding to NFATc1,c2, c3, or c4. Bound and unbound (*free*) CN are shown. The peptide sequences are detailed in Fig. 1. *C*, GST-NFATc2 was employed to bind CN in the presence or in the absence of CaM and in the presence of increasing concentrations of the LxVPc1 peptide. Bound and unbound (*free*) CN are shown.

All of these binding assays were performed in the presence of CaM and calcium, thus mimicking the conditions under which CN is activated *in vivo*. Our results indicated that under these conditions the LxVPc1 peptide was a stronger competitor than the PxIxIT peptides. In the case of PxIxITc2, it has been reported that higher concentrations of peptide are required to block the binding of NFAT to activated CN than those necessary to block the binding to inactive CN (11). To investigate the potential influence of CN activation on its interaction with LxVP, we competed NFATc2 binding to CN with LxVPc1 in the presence or absence of CaM; in these experiments the absence of CaM reduced the potency of the LxVPc1 peptide as a competitor for the CN-NFAT interaction (Fig. 6*C*).

Cross-competition between the CN Binding Sequences of NFATs—The ability of the LxVPc1 peptide to compete CN binding to NFATc2 (Figs. 4–6) was surprising. To investigate this further, we conducted new competition experiments, this time to test the capacity of peptides to compete for CN binding with GST-peptide fusion proteins. The LxVPc1 peptide competed the binding of CN to GST-PxIxITc2, and conversely the PxIxITc2 peptide, as well as VIVIT (a PxIxIT-derived peptide), competed the binding of CN to GST-LxVPc1 (Fig. 7). Given the lack of any clear sequence similarity between these two NFAT

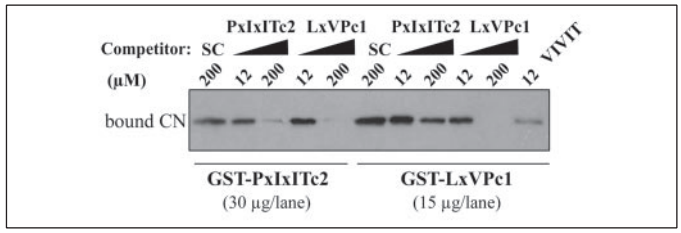

FIGURE 7. **Cross-competition of GST-PxIxITc2-CN or GST-LxVPc1-CN interactions by free PxIxITc2 and LxVPc1 peptides.** GST-peptide fusion proteins containing the PxIxITc2 or LxVPc1 sequence were used to pull-down CN in the presence of free competitor peptides as indicated. The SCRAMBLED peptide (*SC*, 200 μM) was used as negative competitor control, and the effect of VIVIT peptide (12 μM) was also analyzed. To better detect the amount of CN bound to the weaker binding GST-PxIxITc2, the amount of GST-PxIxITc2 employed in these assays was double that of GST-LxVPc1.

motifs, these data suggest that the CN sequences that interact with NFAT PxIxIT and LxVP motifs might be somehow interdependent.

The LxVPc1 Peptide Inhibits the Phosphatase Activity of CN—The results shown in Fig. 6*C* demonstrate that LxVPc1 is a more effective inhibitor peptide of CN-NFAT interaction in the presence of CaM. Under these conditions, the autoinhibitory domain of CN is positioned away from the active center. We therefore considered whether the

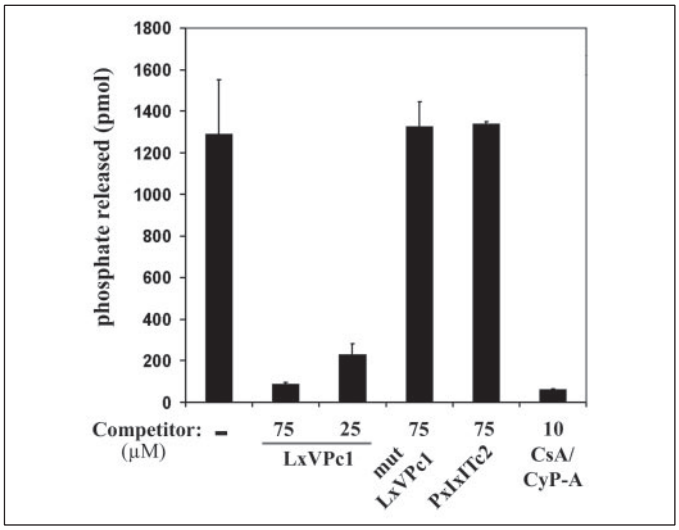

FIGURE 8. **The LxVPc1 peptide is a potent inhibitor of CN phosphatase activity.** The *in vitro* phosphatase activity of CN on the substrate RII phosphopeptide was measured in the presence of different peptides (PxIxITc2, LxVPc1, and mutLxVPc1). The results were compared with that obtained in the presence of 10 μM of the CsA/CyP-A inhibitory complex. The data represent picomoles of free phosphate released during the reaction, and are expressed as the mean and ± S.D. The chart shows the results of one representative experiment of three performed.

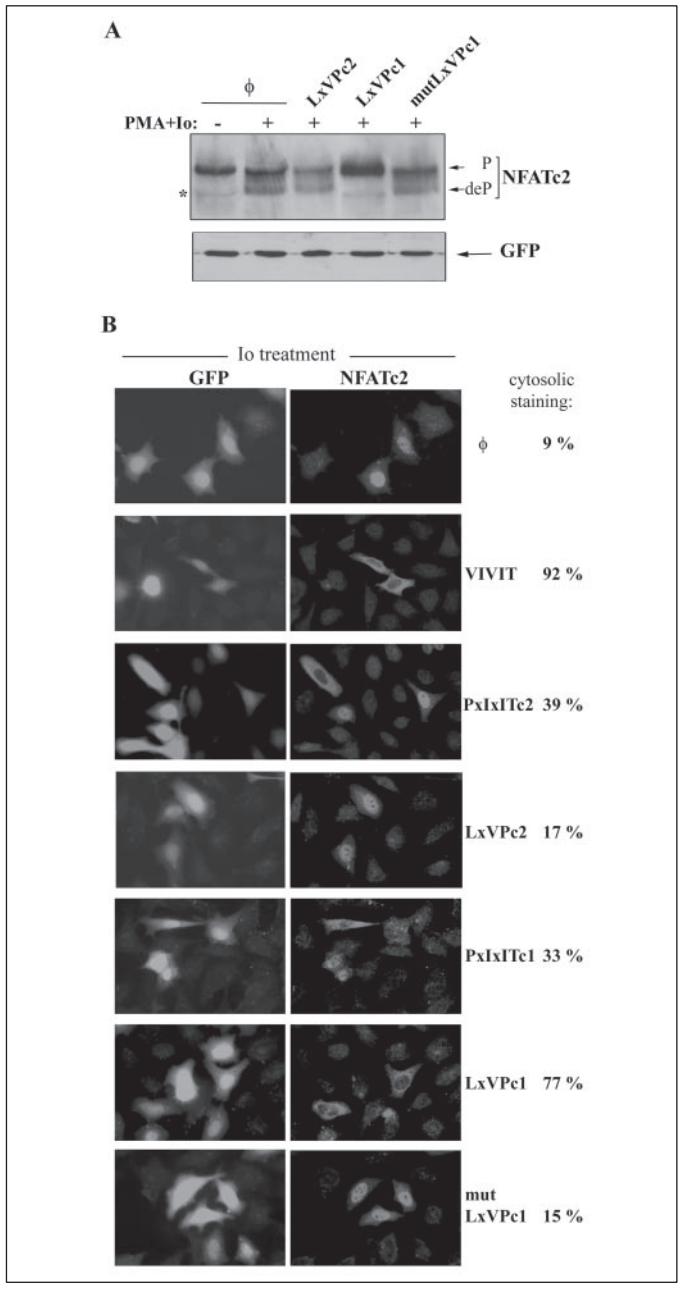

FIGURE 9. **Blockade of NFATc2 regulation by the LxVPc1 peptide *in vivo*.** The NFAT-negative cell line HeLa was co-transfected with constructs encoding HA-tagged wild-type NFATc2 and GFP fusion proteins containing the PxIxIT or LxVP peptides from NFATc2 or NFATc1. The mutant LxVPc1 peptide fused to GFP (mutLxVPc1) was analyzed as a control. *A*, transfected HeLa cells were untreated (−) or stimulated (+) with PMA (20 ng/ml) plus calcium ionophore (1 μM) (*PMA+Io*) for 1 h. Total cell lysates were analyzed by Western blotting with either an anti-HA antibody for NFATc2 detection (*top panel*) or an anti-GFP serum to control for even expression of GFP fusion proteins (*bottom panel*). The electrophoretic mobilities of the *upper* (*P*) and *lower* (*deP*) bands correspond to the phosphorylated and dephosphorylated NFATc2 proteins, respectively. Lysates of cells expressing only the parental GFP protein, bearing no peptide, are shown (*ϕ lanes*). The *asterisk* indicates a nonspecific band. *B*, subcellular localization of NFATc2 in transfected HeLa cells treated with calcium ionophore (*Io*) for 30 min. Panels show representative fields of cells expressing the corresponding GFP-peptide fusion protein (*left*) and the specific immunofluorescence staining for NFATc2 (*right*). The percentage of cells with a cytosolic NFATc2 distribution is indicated (at least 130 cells were counted per transfection).

LxVPc1 peptide might have an effect on CN phosphatase activity. In agreement with previous findings (15, 29), we found that the PxIxITc2 peptide failed to inhibit CN phosphatase activity (Fig. 8). However, the LxVPc1 peptide (but not its mutant version) severely blocked the *in vitro* phosphatase activity of CN. This novel finding suggests either that the LxVPc1 peptide binds close to the CN active site or that the interaction of LxVPc1 with CN alters the conformation of activated CN.

In Vivo Expression of LxVPc1 Peptide Blocks NFATc2 Activation—The ability of the LxVPc1 peptide to both strongly block the CN-NFAT interaction and the CN phosphatase activity prompted us to express it in living cells, to analyze its impact on the *in vivo* regulation of NFATc2. We co-transfected the NFAT-negative HeLa cell line with full-length wild-type NFATc2 and vectors encoding GFP-peptide fusion proteins bearing the LxVP or PxIxIT sites from NFATc1 or NFATc2. GFP-peptide fusion proteins bearing the VIVIT peptide or the mutant LxVPc1 sequence were used as positive and negative inhibition controls, respectively.

Western blot analysis of total cell extracts showed that the expression of GFP-LxVPc1 blocked NFATc2 dephosphorylation induced by increases in intracellular calcium (Fig. 9*A*), whereas the expression of GFP control, GFP-LxVPc2, or GFP-mutLxVPc1 had no effect. However, in apparent contrast to previously published findings (15), we did not detect any significant effect on NFATc2 dephosphorylation when GFP-PxIxITs were expressed (data not shown). Because a potential reason for this discrepancy could be the presence of NFATc2 in GFP-negative cells, we used immunofluorescence to analyze the direct effect of GFP-peptides on NFATc2 nuclear translocation. Control immunofluorescence analysis of non stimulated cells indicated that NFATc2 was in the cytoplasm of cells transfected with the different GFP constructs (data not shown). In most cells transfected with GFP control peptide, NFATc2 was localized in the nucleus after activation with calcium ionophore, with only 9% showing cytosolic NFATc2 staining (Fig. 9*B*). As with NFATc2 dephosphorylation, the greatest inhibitory effect on NFATc2 nuclear translocation was achieved by the expression of GFP-VIVIT and GFP-LxVPc1: 92 and 77% of cells displaying cytosolic staining of NFATc2, respectively. In addition, we observed that the expression of GFP-PxIxITc2 or GFP-PxIxITc1 partially inhibited NFATc2 nuclear translocation: 33–39% of GFP-positive cells displayed a cytosolic localization for NFATc2 upon activation (Fig. 9*B*); this is in agreement with the data published by Aramburu *et al.* (15). These results are

also in agreement with our *in vitro* studies and clearly suggest that the LxVPc1 peptide maintains its ability to interact strongly with CN and/or inhibit CN phosphatase activity *in vivo*, thereby preventing NFATc2 dephosphorylation and nuclear translocation.

DISCUSSION

The identification of the sites on NFAT proteins that interact directly with the phosphatase calcineurin represents an important advance in understanding of the mechanisms that regulate calcium-mediated NFAT activation. In this study we have compared the interaction of NFATc1 and NFATc2 with activated CN *in vitro*. Our semi-quantitative analysis clearly shows that the interaction of CN with NFATc1 is stronger than that with NFATc2. Indeed, NFATc2 significantly increases its ability to interact with CN when its LxVP motif is replaced by the LxVP motif from NFATc1. These differences might be related to different functional roles of each transcription factor in particular cell types or biological processes where both proteins are co-expressed, such as occurs in T cell activation (37) and muscle cell differentiation (33). Our results suggest that in such physiological situations, active CN might preferentially bind to NFATc1, possibly controlling the expression of NFAT-dependent genes in a member-specific fashion.

The low affinity of the PxIxIT sequence for calcineurin in non-stimulated cells appears to be a mechanism to prevent constitutive NFAT activation, and to favor a rapid response to extracellular stimuli (40). In stimulated cells, it has been suggested that CN exposes its active site to increase the strength of the CN-NFAT interaction, thereby facilitating dephosphorylation of the serine/threonine residues within the NFAT regulatory domain (11). However, the identification of a second CN binding motif (LxVP) at the C terminus of the regulatory domains of NFATc1 and NFATc3 suggests that the regulation of CN-NFAT interaction is more complex (17, 31). Because our results suggest that the affinities of the PxIxIT sites in NFATc2 and NFATc1 for CN are similar, the differences between the overall CN binding strengths of these NFAT proteins must reflect the contribution of other CN-interacting motifs. Our competition experiments with peptides based on the LxVP sites from all the NFAT members suggest that NFATc3 and NFATc4 would have a similar strength of interaction with CN to NFATc1. Thus, while PxIxIT is the major CN binding site in NFATc2, the efficient LxVP sites contained in NFATc1, c3 and c4 would contribute to a tighter CN-NFAT interaction.

We have shown that the LxVPc2 peptide is a very weak competitor of CN binding to NFAT, suggesting that the NFATc2-CN interaction would be mainly driven by the PxIxIT motif. The NFATc1 LxVP motif presents a different picture. This peptide bound CN much more efficiently than did the PxIxIT motifs from NFATc1 or NFATc2 (Fig. 3*A*). It also inhibited the *in vitro* interaction of CN with both NFAT proteins, CN phosphatase activity, and the *in vivo* translocation of NFATc2 in activated cells (Figs. 4–6, 8, and 9). The LxVP peptides based on NFATc1, c3 and c4 sequences also proved very efficient competitors of the *in vitro* interaction of CN with NFATc1 or NFATc2. Expression of the LxVPc3 and LxVPc4 peptides in cells might therefore be expected to have an effect on NFATc2 activation similar to what we observed with LxVPc1. However, the LxVP sequence of NFATc3 has been reported to selectively inhibit NFATc3 activation in activated cells, with no effect on NFATc2 (32). These authors used a retroviral construct to infect cells and express the inhibitory peptide, whereas we used cells transiently transfected with a GFP-LxVPc1 plasmid. In our system, complete inhibition of NFATc2 activation was only achieved when LxVPc1 was expressed at high levels. It may be that fine tuning of the exogenous LxVP peptide expression levels could result in a selective, member-dependent blockade of NFAT activation in a given cell type. Alternatively, the different functional behaviors of the LxVPc3 and LxVPc1 peptides reported by Liu *et al.* (32) and ourselves may reflect sequence differences between these binding sites.

We have presented strong evidence that the conserved Leu, Val, and Pro residues in the LxVPc1 motif are essential for the interaction of NFATc1 with CN. However, the fact that the LxVPc2 motif also contains these three amino acids indicates that other residues within this region must take part in the protein-protein interaction. Besides the three conserved residues, only NFATc1, c3, and c4 contain an aromatic amino acid adjacent to the LxVP core (Tyr, Phe, and Tyr, respectively). Another sequence difference is the unique presence of a proline residue adjacent to the carboxyl end of the LxVP core in NFATc2. This results in a pair of consecutive Proline residues, a feature absent from the other NFAT members. These observations suggest that differences in the region flanking the core sequence may account for the different functional behavior of the LxVPc2 site in comparison with the LxVPc1, c3, or c4 sites.

The common method of blocking CN-NFAT signaling is to apply the immunosuppressive drugs CsA and FK506, which inhibit the enzymatic activity of CN (24). These agents must bind to their corresponding cellular partners, cyclophilin A and FKBP12 respectively, to act as immunosuppressant. However these interactions affect not only CN phosphatase activity but also other important biological processes, such as mitochondrial permeability and ryanodine receptor function (41, 42). These CN-independent events may contribute to the severe side effects associated with the clinical use of these drugs. We have shown that low concentrations of the LxVPc1 peptide inhibit CN phosphatase activity. This sequence has been described as a CN binding motif within the NFAT regulatory domain and, in contrast with CsA and FK506, it interacts directly with CN. Therefore, it would be expected that this peptide would exclusively affect CN phosphatase activity. Administration of the LxVPc1 peptide would therefore be expected to have fewer side-effects than treatments with CsA or FK506. In addition, the LxVP peptide could be a useful tool for identifying which CsA and FK506 side effects are unrelated to the inhibition of CN phosphatase activity.

On first view, the different primary sequences of the PxIxIT and LxVP motifs suggest that these two sites would interact with different regions of CN. Indeed, previous CN binding competition assays with GST-peptide fusion proteins of the NFATc1 PxIxIT and LxVP sites suggested that their recognition sites on CN are distinct and non-overlapping (17). However, we have presented data from *in vitro* and *in vivo* studies that show that the NFATc1 LxVP motif can inhibit the interaction of CN with NFATc2, even though the NFATc2 LxVP site appears to have little relevance to its binding with CN. Most significantly, we have also shown that the LxVPc1 and PxIxITc2 peptides can cross-compete for CN binding with GST-peptide fusion proteins bearing the PxIxITc2 and LxVPc1 sequences, respectively. The divergence between our data and the results obtained in competition experiments by Park *et al.* (17) is probably caused by the different experimental conditions used in the binding assays. In our experiments the concentration of CN was 10-fold lower than that used by Park *et al.* (17) whereas the concentration of inhibitory peptides was similar. Moreover, we performed these binding experiments in the presence of CaM, and when we omitted CaM we found that the blocking activity of the LxVPc1 peptide was greatly reduced. Our results suggest that the sequences in CN that interact with LxVPc1 and PxIxIT are interdependent. If these sequences are overlapping (or at least in close proximity or contact), this would enable steric hindrance imposed by the presence of the competitor LxVPc1 peptide bound to CN to impede the interaction of CN with the PxIxIT site.

Another possible scenario would be a sequential model for the NFAT interaction with CN. Our *in vitro* binding experiments were carried out with active CN, and in this situation LxVPc1 peptide competes the CN-NFAT binding more strongly than the PxIxIT peptides. We have observed that in the absence of CaM (thus leaving CN not fully activated) the LxVPc1 peptide is a much less effective competitor of the CN-NFAT interaction. Thus, in the context of full-length proteins, CN would contact first with NFATs through the PxIxIT motif (an interaction that can take place with both active and non active CN). Once CN is activated, the LxVP target sequence would be exposed and the second NFAT binding site would interact with it. In this situation, NFAT would be interacting with CN throughout its two CN binding motifs. The addition of an inhibitory peptide based on the LxVP sequence would then disrupt the interaction between any NFAT member and CN. On the other hand, in addition to the *in vitro* binding experiments showing that the LxVPc1 peptide acts by competing the CN-NFAT interaction, we also found that LxVPc1 is able to inhibit CN phosphatase activity. This suggests that LxVPc1 may bind to CN close to its active site and/or may be affecting the conformation of activated CN. Further experiments would therefore be required to analyze the contribution of this phosphatase inhibitory effect, both on *in vitro* binding and on *in vivo* NFATc2 activation.

The results presented in this study provide important insights into the interaction between NFAT and CN, and are consistent with a model in which the different CN binding characteristics of individual PxIxIT and LxVP sites underlie the distinct activities of NFAT members, and enable different NFAT proteins to influence each others activities in cells where they are co-expressed. Precise identification of the specific sequences of CN targeted by the LxVP site will require detailed structural analysis, but unfortunately efforts to co-crystallize the CN-NFAT complex have so far been unsuccessful. Further crystallographic studies, together with the recent reported data on the interaction of CN with the PxIxIT motif (43, 44) will help to resolve and integrate the unknown aspects of the molecular mechanism underlying the interaction of NFAT with CN.

Acknowledgments—We thank Drs. Claude B. Klee and Arautzazu Alfranca for critical reading and helpful comments on the manuscript, and to Dr. Simon Bartlett for excellent editorial assistance. We thank Drs. I. Crespo, and A. Rao for providing reagents and plasmids. We also thank Dionisio Ureña for technical assistance.

REFERENCES

1. Aramburu, J., Heitman, J., and Crabtree, G. R. (2004) *EMBO Rep.* **5,** 343–348
2. Crabtree, G. R., and Olson, E. N. (2002) *Cell* **109,** (suppl.) S67–S79
3. Horsley, V., and Pavlath, G. K. (2002) *J. Cell Biol* **156,** 771–774
4. Lambrechts, D., and Carmeliet, P. (2004) *Cell* **118,** 532–534
5. Wilkins, B. J., and Molkentin, J. D. (2004) *Biochem. Biophys. Res. Commun.* **322,** 1178–1191
6. Rao, A., Luo, C., and Hogan, P. G. (1997) *Annu. Rev. Immunol.* **15,** 707–747
7. Klee, C. B., Ren, H., and Wang, X. (1998) *J. Biol. Chem.* **273,** 13367–13370
8. Stemmer, P. M., and Klee, C. B. (1994) *Biochemistry* **33,** 6859–6866
9. Wesselborg, S., Fruman, D. A., Sagoo, J. K., Bierer, B. E., and Burakoff, S. J. (1996) *J. Biol. Chem.* **271,** 1274–1277
10. Loh, C., Shaw, K. T., Carew, J., Viola, J. P., Luo, C., Perrino, B. A., and Rao, A. (1996) *J. Biol. Chem.* **271,** 10884–10891
11. García-Cózar, F. J., Okamura, H., Aramburu, J. F., Shaw, K. T., Pelletier, L., Showalter, R., Villafranca, E., and Rao, A. (1998) *J. Biol. Chem.* **273,** 23877–23883
12. Luo, C., Shaw, K. T., Raghavan, A., Aramburu, J., Garcia-Cozar, F., Perrino, B. A., Hogan, P. G., and Rao, A. (1996) *Proc. Natl. Acad. Sci. U. S. A.* **93,** 8907–8912
13. Masuda, E. S., Liu, J., Imamura, R., Imai, S. I., Arai, K. I., and Arai, N. (1997) *Mol. Cell Biol.* **17,** 2066–2075
14. Shibasaki, F., Price, E. R., Milan, D., and McKeon, F. (1996) *Nature* **382,** 370–373
15. Aramburu, J., García-Cózar, F., Raghavan, A., Okamura, H., Rao, A., and Hogan, P. G. (1998) *Mol. Cell* **1,** 627–637
16. Chow, C. W., Rincón, M., and Davis, R. J. (1999) *Mol. Cell Biol.* **19,** 2300–2307
17. Park, S., Uesugi, M., and Verdine, G. L. (2000) *Proc. Natl. Acad. Sci. U A* **97,** 7130–7135
18. Zhu, J., Shibasaki, F., Price, R., Guillemot, J. C., Yano, T., Dötsch, V., Wagner, G., Ferrara, P., and McKeon, F. (1998) *Cell* **93,** 851–861
19. Shaw, J. P., Utz, P. J., Durand, D. B., Toole, J. J., Emmel, E. A., and Crabtree, G. R. (1988) *Science* **241,** 202–205
20. Macián, F., López-Rodríguez, C., and Rao, A. (2001) *Oncogene* **20,** 2476–2489
21. Macián, F., García-Cózar, F., Im, S. H., Horton, H. F., Byrne, M. C., and Rao, A. (2002) *Cell* **109,** 719–731
22. Serfling, E., Berberich-Siebelt, F., Avots, A., Chuvpilo, S., Klein-Hessling, S., Jha, M. K., Kondo, E., Pagel, P., Schulze-Luehrmann, J., and Palmetshofer, A. (2004) *Int. J. Biochem. Cell Biol.* **36,** 1166–1170
23. Macian, F. (2005) *Nat. Rev. Immunol.* **5,** 472–484
24. Liu, J., Farmer, J. D., Jr., Lane, W. S., Friedman, J., Weissman, I., and Schreiber, S. L. (1991) *Cell* **66,** 807–815
25. Crabtree, G. R., and Clipstone, N. A. (1994) *Annu. Rev. Biochem.* **63,** 1045–1083
26. Liu, J. (1993) *Immunol. Today* **14,** 290–295
27. Rao, A. (1994) *Immunol. Today* **15,** 274–281
28. Kiani, A., Rao, A., and Aramburu, J. (2000) *Immunity* **12,** 359–372
29. Aramburu, J., Yaffe, M. B., López-Rodríguez, C., Cantley, L. C., Hogan, P. G., and Rao, A. (1999) *Science* **285,** 2129–2133
30. Roehrl, M. H., Kang, S., Aramburu, J., Wagner, G., Rao, A., and Hogan, P. G. (2004) *Proc. Natl. Acad. Sci. U. S. A.* **101,** 7554–7559
31. Liu, J., Masuda, E. S., Tsuruta, L., Arai, N., and Arai, K. (1999) *J. Immunol.* **162,** 4755–4761
32. Liu, J., Arai, K., and Arai, N. (2001) *J. Immunol.* **167,** 2677–2687
33. Abbott, K. L., Friday, B. B., Thaloor, D., Murphy, T. J., and Pavlath, G. K. (1998) *Mol. Biol. Cell* **9,** 2905–2916
34. Boss, V., Abbott, K. L., Wang, X. F., Pavlath, G. K., and Murphy, T. J. (1998) *J. Biol. Chem.* **273,** 19664–19671
35. Ferrari, D., Stroh, C., and Schulze-Osthoff, K. (1999) *J. Biol. Chem.* **274,** 13205–13210
36. Johnson, E. N., Lee, Y. M., Sander, T. L., Rabkin, E., Schoen, F. J., Kaushal, S., and Bischoff, J. (2003) *J. Biol. Chem.* **278,** 1686–1692
37. Lyakh, L., Ghosh, P., and Rice, N. R. (1997) *Mol. Cell Biol.* **17,** 2475–2484
38. Van Rooij, E., Doevendans, P. A., De Theije, C. C., Babiker, F. A., Molkentin, J. D., and De Windt, L. J. (2002) *J. Biol. Chem.* **277,** 48617–48626
39. Gómez del Arco, P., Martínez-Martínez, S., Maldonado, J. L., Ortega-Pérez, I., and Redondo, J. M. (2000) *J. Biol. Chem.* **275,** 13872–13878
40. Hogan, P. G., Chen, L., Nardone, J., and Rao, A. (2003) *Genes Dev.* **17,** 2205–2232
41. Molkentin, J. D. (2001) *Circ. Res.* **88,** 1220–1222
42. Bandyopadhyay, A., Shin, D. W., Ahn, J. O., and Kim, D. H. (2000) *Biochem. J.* **352,** 61–70
43. Li, H., Rao, A., and Hogan, P. G. (2004) *J. Mol. Biol.* **342,** 1659–1674
44. Rodríguez, A., Martínez-Martínez, S., López-Maderuelo, M. D., Ortega-Pérez, I., and Redondo, J. M. (2005) *J. Biol. Chem.* **280,** 9980–9984

Mechanisms of Signal Transduction:

Blockade of NFAT Activation by the Second Calcineurin Binding Site

Sara Martínez-Martínez, Antonio Rodríguez, Maria Dolores López-Maderuelo, Inmaculada Ortega-Pérez, Jesús Vázquez and Juan Miguel Redondo

J. Biol. Chem. 2006, 281:6227-6235.
doi: 10.1074/jbc.M513885200 originally published online January 6, 2006